

FERMILAB BOOSTER BEAM COLLIMATION AND SHIELDING*

N.V. Mokhov, A.I. Drozhdin, P.H. Kasper, J.R. Lackey, E.J. Prebys, R.C. Webber
FNAL, Batavia, IL 60510, USA

May 7, 2003

Abstract

The beam power in the upgraded Booster at 8 GeV and 10 Hz will be 64 kW. Beam loss can result in high radiation loads in the ring. The purpose of a new beam halo cleaning system is to localize proton losses in specially shielded regions. Calculations show that this 2-stage collimation system will localize about 99% of beam loss in straight sections 6 and 7 and immediately downstream. Beam loss in the rest of the machine will be on average 0.1 W/m. Local shielding will provide tolerable prompt and residual radiation levels in the tunnel, above the tunnel at the surface and in the sump water. Results of thorough MARS calculations are presented for a new design which includes shielding integrated with the collimators, motors and controls ensuring a high performance and facilitating maintenance. First measurements of the collimation efficiency are presented.

*Presented paper at the *2003 Particle Accelerator Conference*, Portland, OR, May 12-16, 2003

FERMILAB BOOSTER BEAM COLLIMATION AND SHIELDING*

N.V. Mokhov[†], A.I. Drozhdin, P.H. Kasper, J.R. Lackey, E.J. Prebys, R.C. Webber
FNAL, Batavia, IL 60510, USA

Abstract

The beam power in the upgraded Booster at 8 GeV and 10 Hz will be 64 kW. Beam loss can result in high radiation loads in the ring. The purpose of a new beam halo cleaning system is to localize proton losses in specially shielded regions. Calculations show that this 2-stage collimation system will localize about 99% of beam loss in straight sections 6 and 7 and immediately downstream. Beam loss in the rest of the machine will be on average 0.1 W/m. Local shielding will provide tolerable prompt and residual radiation levels in the tunnel, above the tunnel at the surface and in the sump water. Results of thorough MARS calculations are presented for a new design which includes shielding integrated with the collimators, motors and controls ensuring a high performance and facilitating maintenance.

BEAM COLLIMATION

With the construction of an 8 GeV target station for the 5 Hz MiniBooNE neutrino beam and rapid multi-batch injection into the Main Injector for the NuMI experiment, the demand for Booster protons is increased dramatically at Fermilab. This implies serious constraints on beam losses in the machine. The beam power in the Booster at 8 GeV with 5×10^{12} ppp at 10 Hz will be 64 kW. Assuming that 30% of the beam is lost at injection and 2% at top energy, 0.96 kW (at 0.4 GeV) and 1.28 kW (at 8 GeV) of beam loss are distributed around the ring with a beam loss rate of 13-60 W/m in the RF cavities. The corresponding residual radiation levels inside the tunnel, in sump water and the prompt radiation levels outside the tunnel shielding would substantially exceed tolerable limits.

In order to control beam loss and corresponding radiation levels around Booster so as to avoid radiation damage to sensitive components (cables, connectors etc) and minimize exposures to personnel and environment, particularly in high-maintenance areas (RF stations), one needs to intercept those protons that are doomed to be lost and contain them in a well shielded location. The purpose of the beam halo cleaning system proposed in Ref. [1] is to localize proton losses in sections 6 and 7 which are far from the engineering, support and office buildings.

A 2-stage collimation system is proposed with thin horizontal and vertical carbon or tungsten foils (section 5) followed by secondary collimators (sections 6 and 7). Foils are placed at the edge of the circulating beam after injection. Secondary collimators are positioned with a 0.5σ offset with respect to the foils at phase advances that are op-

timal to intercept most of particles out-scattered from the foils during the first turn after the halo interaction with the foils (37° and 154° horizontal, and 20° and 127° vertical).

It was shown in Ref. [1] that the highest collimation efficiency is achieved if the scatterer thickness is changed during the cycle from 0.003 mm to 0.1 mm for tungsten or from 0.15 mm to 5.4 mm for carbon. This can be done by rotation of a wedge disk. Currently installed are two 0.3-mm carbon foils. Fig. 1 shows recent measurements of beam loss rates in the Booster ring as a difference between beam loss monitor readings without any collimators and with the vertical primary collimator in. As expected, losses are decreased everywhere except near the L6 section – a location where the secondary collimators will be installed to intercept the protons scattered in the primary collimators.

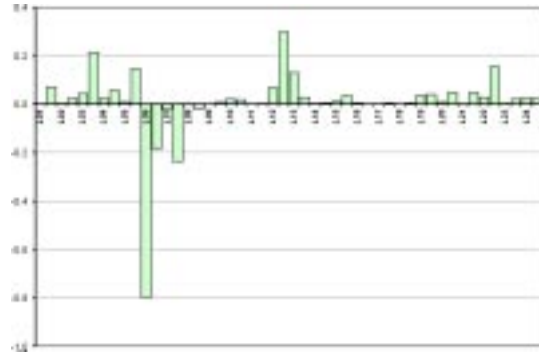


Figure 1: Difference in BLM readings around the ring without and with the L5 vertical primary collimator.

The jaws of the secondary collimators L6A (H), L6B (V+H) and L7 (V+H) are 0.6-m long stainless steel. Such a system would localize about 99% of beam loss in these three regions and immediately downstream. Beam loss in the rest of the machine is on average 0.1 W/m, with several peaks of ~ 1 W/m. Beam loss rates, calculated for a 5×10^{12} proton beam at 10 Hz as a fraction of the total beam intensity, are

- At 8 GeV: 1% or 5×10^{11} p/s in L6 (two thirds on L6A and one third on L6B), and 1% in L7 and in short regions downstream of L6 and L7.
- At 0.4 GeV: 20% or 10^{13} p/s in L6 (two thirds on L6A and one third on L6B), and 10% in L7 and in short regions downstream of L6 and L7.

These results are based on STRUCT simulations performed for the Booster lattice without injection and extraction bumps. Recent studies reveal that large focusing effects of these rectangular bump magnets change the β -functions and dispersion, and may affect the collimation system efficiency calculated.

* Work supported by the Universities Research Association, Inc., under contract DE-AC02-76CH03000 with the U. S. Department of Energy.

[†] mokhov@fnal.gov

INTEGRATED SYSTEM

Full-scale Monte Carlo hadronic and electromagnetic shower simulations in the collimators, lattice elements, shielding, tunnel and surrounding soil are done with MARS14 [2] code. The following constraints were taken into account while developing the optimal collimator-shielding system:

- Prompt dose equivalent at peak, 13.5 feet of dirt above the tunnel, is below 0.05 mSv/hr (1 Sv = 100 rem).
- Activation of water in the sumps is within the allowed limits for surface discharge. This corresponds to a star density, averaged over the gravel around the tunnel, of less than $4000 \text{ cm}^{-3}\text{s}^{-1}$.
- Activation of the outer surfaces that are accessible to personnel allows hands-on maintenance with a residual contact dose rate below 1 mSv/hr after 30-day of irradiation and 1-day of cool off.
- Accumulated absorbed dose in cables, motors, and instrumentation is below the 20-year lifetime limits.
- Air activation and water activation in nearby LCW pipes is low.

The original design [1] consisted of L-shaped copper jaws brazed to a beam pipe. Stands and motors were designed to allow lots of room to stack steel shielding. There were, necessarily, rather large gaps between the jaws and shielding allowing radiation to escape the core, activate air and increasing the shielding dimensions. To access the collimator itself in the event of a catastrophic failure would require removing the shielding and exposing a very hot object. The final solution was an integrated collimator-shielding system. In this design, all failure prone components are outside the shielding. This module is rather compact (approximately $1 \times 1 \times 1 \text{ m}^3$ outside) and uniform, with no cracks and gaps, eliminating the air activation problem. Because of the tight integration of the collimator and shielding steel, both the collimator and the surrounding shielding move as a unit. The actuators are to be sized to move the 11.6 ton block, a typical weight for remotely operated magnet stands.

The mechanical-electrical design took the following mechanical specifications into account:

- The apertures do not occlude any beam when in the garage position.
- They can be remotely translated by 1.5 inches both horizontally and vertically.
- They can be remotely positioned to $\pm 1 \text{ mm}$.
- Their orientation can be remotely corrected for pitch and yaw misalignments of up to $\pm 10 \text{ mrad}$.
- The time required to move them from fully in to fully out should be no longer than a few minutes.
- It should be possible to reliably disable the motion controls.
- All sensitive components should be serviceable without major disruptions to the program.

- It should be possible to completely remove them from the tunnel even after many months of beam.

MARS MODELING AND RESULTS

The system parameters were thoroughly optimized via MARS14 calculations. Fragment of a finalized model are shown in Fig. 2 and 3. All the radiation limits and design constraints of the previous section were taken into account.

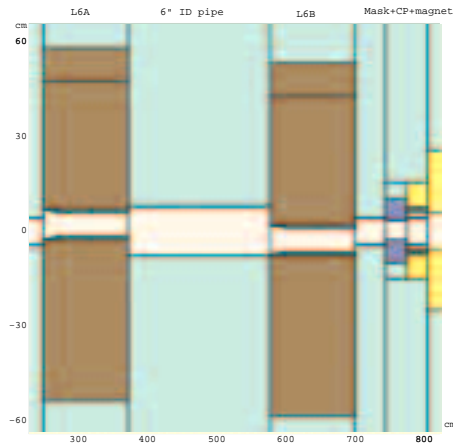


Figure 2: A fragment of the L6 integrated system.

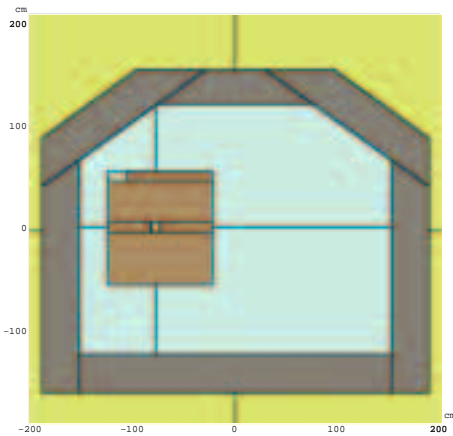


Figure 3: A cross-section of tunnel at L6B.

Based on the calculated 3D energy deposition profiles in the L6A and L6B collimator jaws and shielding, an ANSYS thermal and stress analysis was performed. It was found that no cooling is needed for normal operation and that the maximum steady-state temperature would be 60°C . It was also calculated that there should be no mechanical problems caused by the differential thermal expansion of the jaws and shielding. In an accident case in which the full 8-GeV beam is lost on the collimator, the jaw will withstand 25 pulses over 2.5 s.

Longitudinally, the peak radiation fields were found to occur at the upstream end of the L6B collimator. Fig. 4 shows a vertical profile of prompt dose from 8-GeV beam scraping, in a ± 1 m band located at that peak. The cumulative maximum dose on the surface after 13.5 feet of dirt is 0.0125 mSv/hr, i.e. four times below the limit. Scraping at the injection energy of 0.4 GeV gives 20% of this value. Activation of water in the sumps is caused predominantly by spallation reactions above 50 MeV (*stars*). A horizontal profile of star density from a 8-GeV beam scraping, in a ± 1.6 m band is shown in Fig. 5. The cumulative average star density immediately outside the tunnel walls is $1163 \text{ cm}^{-3}\text{s}^{-1}$, i.e. 3.5 times below the limit. Scraping at injection gives 30% of this value. In reality, the margin is 2 to 3 times better if one averages over the gravel fill surrounding the tunnel.

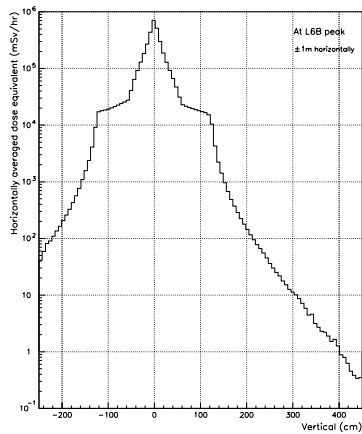


Figure 4: Prompt dose vertical profile.

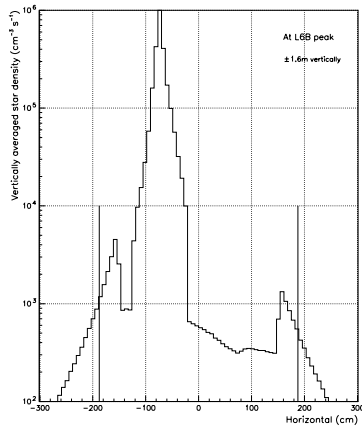


Figure 5: Star density horizontal profile.

Fig. 6 shows a 2D distribution of residual dose at the upstream end of the L6B collimator-shielding for 8-GeV beam scraping. The inner parts are very hot: up to 1 Sv/hr at jaws. Cumulative dose rate on the shielding outside ranges from 0.3 to 1 mSv/hr. Scraping at injection gives 15-25% of these values. The maximum contact dose on the aisle side of the L6B module is right on the limit (Fig. 7). The maximum dose on the 6-inch bare beam-pipes right after L6A and L6B is 40 mSv/hr. The dose on the outside

of the correction package (CP) immediately upstream of the main magnet varies azimuthally from 5 to 40 mSv/hr, while on the outside of the first main magnet – from 2 to 10 mSv/hr.

Yearly absorbed dose at the L6B longitudinal peak is about 20 MGy/yr (1 Gy = 100 rad) on the jaws, 40 kGy/yr on shielding outside and up to 10 kGy/yr at walls, ceiling and floor. The maximum absorbed dose in the CP inner coils varies azimuthally from 0.3 to 4 MGy/yr that can reduce their lifetime. It was found that a simple 30-cm long steel mask (7.6 cm ID, 30 cm OD) between L6B and CP reduces the accumulated and residual doses by up to a factor of four.

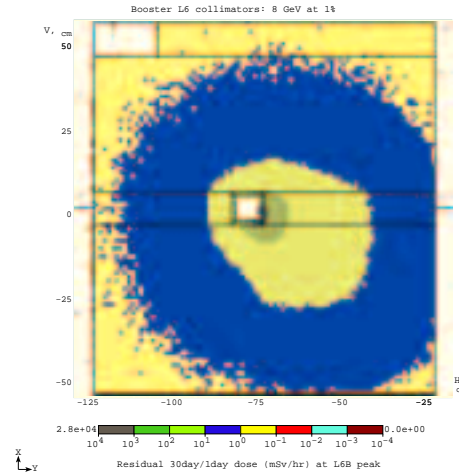


Figure 6: Contact residual dose rate at L6B after 30-day scraping at 8 GeV and 1-day cooling.

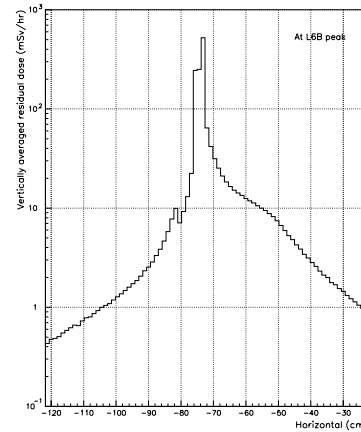


Figure 7: Horizontal profile of residual dose rate at L6B.

REFERENCES

- [1] A.I. Drozhdin, P.H. Kasper, O.E. Krivosheev, J.R. Lackey, N.V. Mokhov, M. Popovic, R.C. Webber, *Proc. of the 2001 Part. Accel. Conf.*, Chicago, June 2001, p. 2569.
- [2] N.V. Mokhov, “The MARS Code System User’s Guide”, Fermilab-FN-628 (1995); N.V. Mokhov, “Status of MARS Code”, Fermilab-Conf-03/053 (2003); <http://www-ap.fnal.gov/MARS/>.